Limiting effect of self-shading on the height of *Tradescantia fluminensis* mats

Michael J. Plank[1,2], Nick Stringer[1], Shona L. Lamoureaux[3], Graeme W. Bourdôt[3], Alex James[1,2]

1. School of Mathematics and Statistics, University of Canterbury, Christchurch, New Zealand
2. Te Pūnaha Matatini, a New Zealand Centre of Research Excellence
3. AgResearch Limited, Lincoln, New Zealand

Abstract

Tradescantia fluminensis is an invasive plant species in New Zealand, Australia and parts of the United States. It reproduces vegetatively and can grow to form dense mats up to 60 cm deep. Growth is limited by available light and shading is one of the few effective methods of control. In this paper, we develop a dynamic model of a vertical cross-section of a *T. fluminensis* mat, capturing vertical variation in its biomass and internal light intensity. We measure both variables at different heights in experimental mats of the species and use these data to parameterize the model. The model produces realistic vertical biomass and light intensity profiles. We show that the mat grows to a steady state biomass that depends only on: (i) the light absorption coefficient, which we estimate from experimental data, and (ii) the ratio of photosynthesis to respiration rate. This steady state undergoes a transcritical bifurcation; when the ambient light intensity falls below a critical level, the biomass shrinks to zero and the mat cannot survive.

Keywords: plant biomass; energy balance; invasive species; light intensity; photosynthesis.

Introduction

Tradescantia fluminensis Vell. (Scott & Priestley, 1925) is a ground-covering perennial herb native to South America that has established in native forest remnants in New Zealand, Australia and south eastern states of the United States. In New Zealand, *T. fluminensis* has few natural predators and, as a result, can grow to much higher biomass than in its native range (Kelly & Skipworth, 1984a). At these higher biomass levels*, T. fluminensis* forms a dense mat, up to 60 cm deep, which inhibits the growth of native seedlings, preventing native forest regeneration and leading to reduced invertebrate density (Toft, Harris, & Williams, 2001) and altered nutrient availability (Standish, 2004) and soil microfauna (Yeates & Williams, 2001). In New Zealand, *T. fluminensis* only spreads vegetatively. Its stems are easily broken and even small segments of plant have a high probability of survival and regrowth (Kelly & Skipworth, 1984a). Its prolific growth, lack of natural predators and ability to stifle regenerating native plants has led to *T. fluminensis* being included on New Zealand's National Pest Plant Accord (MPI, 2013), meaning it is banned from sale, propagation and distribution.

The distribution of *T. fluminensis* is highly correlated with anthropogenic variables (Butcher & Kelly, 2011). It is also light-sensitive: *T. fluminensis* biomass is positively correlated with light intensity, with the highest densities being found at light levels of up to 30–50% of open ground. For light levels above 50% of open ground, the standing crop is still high but not related to light intensity (Maule et al., 1995). The abundance and richness of native seedlings decreases with increasing *T. fluminensis* biomass (McAlpine et al., 2015; Standish, 2002). This is thought to be a result of decreased light levels; below a mat of complete *T. fluminensis* cover, light level is reduced to less than 1%. Newly germinated seed are found underneath *T. fluminensis* ground coverage but most of these do not develop into seedlings (Kelly & Skipworth, 1984a; Standish, 2002).

Control of *T. fluminensis* in New Zealand is mostly either by herbicide application or hand weeding. Neither of these methods can achieve complete removal and prevent regrowth (Kelly & Skipworth, 1984b), so artificial shading has been suggested as another possible control method (Standish, 2002). Shading is not intended to remove the plant entirely but to reduce the biomass to a level at which native woody plants can overtop and outcompete *T. fluminensis*. More recently, biological control methods including three species of criocerine beetles and a fungus have been tested for release in New Zealand (Fowler et al., 2013).

A demographic model for the life-cycle of plants in the Commelinaceae family, of which *T. fluminensis* is a member, has been proposed (Burns, 2008). However, this is not applicable for *T. fluminensis* in invasive areas, such as Australia and New Zealand, where the plant does not seed and only spreads vegetatively. Instead, mathematical models of *T. fluminensis* have focused on growth of the mat via the branching of nodes to form new growing tips and stems. For example, James et al. (2015) derived a model for the number of tips and nodes in a plant and used this to investigate the effectiveness of control methods targeting different parts of the plant. This model was based on ordinary differential equations describing change in the number of plant tips and nodes over time and was parameterized with data from field experiments. Spatially unstructured models, such as those referred to above, only capture aggregate properties of the plant and cannot account for any structure or spatial variation within the mat. Hogan & Myerscough (2017) modelled the density of tips and leaves and investigated how these spread horizontally during mat growth. This model included self-shading via a simple equation representing branching rate as a function of leaf density, but did not explicitly model vertical variation in plant biomass or light intensity. Other models of plant growth and architecture exist in the literature (e.g. Jaeger & De Reffye (1992), Prusinkiewicz (2004), Yan et al. (2004), Sellier et al. (2011)) but most of these do not link growth and structure with the degree of light absorption by plant biomass. Conversely, there are numerous models of the effects of shading on plant populations (e.g.

Brunner (1998), Perry et al. (2003), Vance & Nevai (2007), Adams et al. (2013)), but these focus on the effects of shading by one plant on another as opposed to self-shading.

In this study, we develop a mathematical model for the growth of a *T. fluminensis* mat in the vertical direction that explicitly links vertical variations in plant biomass and variations in internal light intensity due to absorption. We collected empirical data on biomass and light intensity from *T. fluminensis* plants grown under glasshouse conditions and used these to parameterize the model. By calculating a height-dependent energy balance between photosynthetic biomass production and metabolism, the model predicts the resulting biomass-height profile and the steady state height of the mat. We use the model to investigate the outcomes of different scenarios, such as high versus low ambient light or metabolic rate. This allows us to calculate the threshold ambient light intensity below which the mat is predicted to die.

Experimental methods

Four replicate *T. fluminensis* mats were grown in a glasshouse at the University of Canterbury, Christchurch, New Zealand between November 2015 and June 2016. Each of the four replicates consisted of four *T. fluminensis* plants, each in a 50 cm by 25 cm by 5cm high rectangular pot containing 5 cm depth of potting mix. The four pots in each replicate were arranged in a two by two configuration. A rectangular container, extending to a height of 40 cm above the surface of the potting mix, was placed around the pots to contain the plants as they grew. During the experimental period, the plants were watered daily by an automated sprinkler system. Over time, the four plants in each of the replicates coalesced and became indistinguishable, forming a single 100 cm by 50 cm mat of up to 40 cm in height.

At the end of the experiment, in June 2016, the light intensity and biomass profile within each of the four replicate mats were measured as follows. A light meter (Onset Computer Corporation HOBO UA-002-64 Pendant Temp/Light version 1.0.8, Serial Number 9742171) was used to measure light intensity (in lux) at four different heights within the central portion of the mat created by the four coalesced plants. The light meter automatically logged light intensity at 1 s intervals. Each measurement was obtained by holding the light meter stationary for a period of 20 s and averaging the 20 logged intensities**.** The first such measurement was made on the surface of the mat, which was at a height of 40 cm above ground level. Subsequent light measurements were then made at heights of 30, 20, 10 and 0 cm above ground level. To obtain light intensity relative to ambient, each of the four measurements within the mat was divided by the surface measurement made at the start (top) of the sequence. This sequence of measurements (heights 40, 30, 20, 10, 0 cm) was immediately repeated three times, giving a total of three relative light intensity measurements at each height and for each replicate mat.

After the light intensity measurements were complete, each of the four mats was cut into four horizontal layers of 10 cm thickness (Fig. 1a) and the biomass in each layer collected and placed in paper bags. Prior to this, any excess biomass flowing over the sides of the container was removed using scissors to ensure that each harvested layer had the same horizontal area (100 cm × 50 cm). Bags of biomass were dried in an oven at approximately 80°C for two weeks and then weighed. The bags were then weighed and their masses deducted to derive the dry plant biomass. As each layer consisted of the biomass in a 0.5 m^2 (100 cm × 50 cm) horizontal cross-section of the mat, the biomass measurements were divided by 0.5 to obtain the biomass per m^2 of horizontal cross-sectional area. Data are provided in Supplementary Material Table S1.

Experimental results

The measured biomass in the 100 cm × 50 cm × 10 cm layers ranged from a minimum of 116.66 g (mat 3, 30-40 cm height) to a maximum of 455.17 g (mat 1, 0-10cm height). This corresponds to a range in biomass per unit volume of 2333.2 g m^{-3} to 9103.4 g m^{-3}. In each of the four mats, the biomass per unit volume decreased with height from an average of 7580 g m^{-3} at 0-10 cm height to 2550 g m^{-3} at 30-40 cm height. The complete dataset is provided in Supplementary Table S1.

Figure 1b shows the relationship between relative light intensity l at a particular height and the total dry biomass w above that height (calculated by summing the biomass per unit horizontal area in the layers above the height at which the light intensity measurement was made). Note that biomass above height h, rather than height itself, is the relevant variable to use because light intensity will be higher in a low-density mat than in a high-density mat at the same height. A relationship of the form $\log(l) = -\mu w$ was fitted to the data using least squares regression (dashed blue line in Fig. 1b). The light absorption coefficient μ was estimated as $\mu = 0.00334$ m^2 g^{-1} ($p < 0.001, r^2 = 0.57$).

Mathematical model

We develop a model that captures the structure of a *T. fluminensis* mat by quantifying the vertical profiles of biomass and light intensity relative to ambient light intensity at the surface of the mat. We assume that the mat is horizontally homogeneous and only varies in the vertical direction. Horizontal growth of the plants making up the mat may take place at the edges of the mat but this is ignored. This assumption effectively reduces the problem to a one-dimensional model with height h as the independent variable (Fig. 2). We divide the mat into N thin layers, each of equal thickness δh. The model output is the biomass per unit volume $\rho_i(t)$ in layer i at time t.

The experimental results show that plant biomass is denser at deeper levels within the mat. We hypothesize that this is primarily due to compression of the mat by its own weight, which is consistent with qualitative empirical observations. We model this by assuming that there is a maximum biomass per unit volume in layer i, K_i, which is a linearly increasing function of the total biomass above layer i:

$$K_i = c_0 + c_1 \delta h \sum_{j=i}^{N} \rho_j. \qquad (1)$$

Here, c_0 is the maximum biomass per unit volume of the upper, uncompressed layers of the mat and c_1 is the extent to which maximum biomass per unit volume increases with depth as a result of compression (i.e. the compressibility of the mat).

Incident light is absorbed by the mat as it penetrates downwards. The light intensity reaching layer i, relative to ambient light intensity, is taken from the experimental relationship $l_i = \exp(-\mu \delta h \sum_{j=i}^{N} \rho_j)$, where μ (with dimensions area per unit mass) is the light absorption coefficient.

We consider two mechanisms that change the biomass in a given layer: settlement, in which biomass moves from one layer to the layer immediately below as a result of compression; and biomass production/decay which is calculated via an energy balance between photosynthesis and metabolism.

Settlement. Biomass settles from layer $i+1$ into layer i at a rate proportional to the biomass per unit volume ρ_{i+1} in layer $i+1$ and the space available in layer i, $1-\rho_i/K_i$. Hence the net change in biomass per unit volume $\delta\rho_{i_c}$ in layer i in a short time step δt due to settlement is

$$\delta\rho_{i_c} = \frac{\lambda_s}{\delta h}\left(\rho_{i+1}\left(1-\frac{\rho_i}{K_i}\right) - \rho_i\left(1-\frac{\rho_{i-1}}{K_{i-1}}\right)\right)\delta t,$$

where λ_s is the settlement rate coefficient (with dimensions distance per unit time). The division by the layer thickness δh ensures the model is insensitive to the choice of δh, provided it is small.

Biomass production/decay. This mechanism is calculated at the level of the entire mat and its output is then apportioned amongst the appropriate layers. Energy available to the plants comprising the mat comes from photosynthesis and the rate of photosynthesis in a given layer is assumed to be proportional to the product of the biomass and the light intensity in that layer. Hence the total rate of biomass production P (per unit area per unit time) is given by

$$P = \lambda_p\,\delta h\sum_{i=1}^{N}\rho_i l_i,$$

where λ_p (dimensions time^{-1}) is the photosynthesis rate coefficient. The value of λ_p will be proportional to the ambient or external light intensity, so by varying this parameter we will explore the effect of ambient light intensity, possibly induced by artificial shading, on model outcome.

Energy is required for basic metabolic processes and maintenance (Cannell & Thornley, 2000). We assume that the biomass demand due to respiration P_r (per unit area per unit time) is proportional to the total biomass:

$$P_r = k\,\delta h\sum_{i=1}^{N}\rho_i.$$

Here k (dimensions time^{-1}) is the respiration rate coefficient. Excess energy not used for respiration is used for growth. If the excess energy is negative then the mat is not able to maintain itself and it decays at a rate proportional to the energy deficit. To capture this energy balance, we define the net biomass production rate P_g (per unit area per unit time) as

$$P_g = P - P_r = \delta h\left(\lambda_p\sum_{i=1}^{N}\rho_i l_i - k\sum_{i=1}^{N}\rho_i\right)$$

If $P_g > 0$ the mat is growing. This overall net increase in biomass must then be apportioned across the layers. This is done by assuming that new growth into layer i occurs from the layer immediately below and is proportional to the biomass per unit volume in the layer below, ρ_{i-1}, the light available in the layer below, l_{i-1}, and the space available, $1-\rho_i/K_i$, in layer i. Hence, growth is partitioned into layer i in proportion to $\rho_{i-1}l_{i-1}(1-\rho_i/K_i)$.

If $P_g < 0$, the mat undergoes biomass decay due to the energy deficit. Field observations show that most biomass loss occurs from the basal part of the plant closest to the ground (James et al., 2015). We therefore apply the biomass loss term only to the part of the mat below height h_d. The resultant change in biomass per unit volume $\delta\rho_{i,g}$ due to growth or decay in layer i in a short time step δt is

$$\delta\rho_{i,g} = \frac{P_g \delta t}{\delta h} \begin{cases} \dfrac{\rho_{i-1} l_{i-1}(1-\rho_i/K_i)}{\sum_{j=1}^{N} \rho_{j-1} l_{j-1}\left(1-\rho_j/K_j\right)}, & \text{if } P_g > 0, \\ \dfrac{U(h_d/\delta_h - i)\rho_i}{\sum_{j=1}^{h_d/\delta h} \rho_j}, & \text{if } P_g < 0, \end{cases}$$

where U is the Heaviside function**.** In the case of a net energy deficit ($P_g < 0$), this term distributes the biomass loss in proportion to the biomass in each of the layers below height h_d.

Combining the settlement and biomass growth/decay terms above and letting the time step $\delta t \to 0$, we obtain a system of differential equations for the biomass per unit volume ρ_i in layers $i = 2, \dots N$:

$$\frac{d\rho_i}{dt} = \frac{\lambda_s}{\delta h}\left(\rho_{i+1}(1-\rho_i/K_i) - \rho_i(1-\rho_{i-1}/K_{i-1})\right) + \frac{P_g}{\delta h} \begin{cases} \dfrac{\rho_{i-1} l_{i-1}(1-\rho_i/K_i)}{\sum_{j=1}^{N} \rho_{j-1} l_{j-1}\left(1-\rho_j/K_j\right)}, & \text{if } P_g > 0, \\ \dfrac{U(h_d/\delta_h - i)\rho_i}{\sum_{j=1}^{h_d/\delta h} \rho_j}, & \text{if } P_g < 0. \end{cases} \quad (2)$$

For the layer closest to the ground there is no biomass loss due to settlement and no biomass increase due to growth (since growth occurs from the layer below). Hence for ρ_1, we get a separate differential equation:

$$\frac{d\rho_1}{dt} = \frac{\lambda_s}{\delta h}\rho_2(1-\rho_1/K_1) + \begin{cases} 0, & \text{if } P_g > 0, \\ \dfrac{P_g \rho_1}{\delta h \sum_{j=1}^{h_d/\delta h} \rho_j}, & \text{if } P_g < 0. \end{cases} \quad (3)$$

Initial conditions and parameter values. For numerical simulations of the model, initial conditions and parameter values need to be specified. Based on the experimental biomass measurements, we set $c_0 = 0.25\rho_{\max}$ where $\rho_{\max} = 9103.4\ \mathrm{g\ m^{-3}}$ was the highest recorded biomass per unit volume. This means that the upper, uncompressed layers of the mat can grow to a biomass that is 25% of the maximum recorded. We set $c_1 = 3.47\ \mathrm{m^{-1}}$, which means that the maximum biomass per unit volume in a mat of 40 cm height is equal to $\rho_{\max}$. The photosynthesis and respiration rate constants λ_p and k are phenomenological parameters that cannot be measured directly. These parameters were chosen to make the model output comparable to the experimental observations (i.e. a mat which grows to approximately 0.4 m in height in around 200 days). The values used ($\lambda_p = 0.1$ day^{-1} and $k = 0.015$ day^{-1}) imply that a unit of biomass can, in completely unshaded conditions, photosynthesize 10% of its own mass per day, and has a respiration cost of 1.5% of its own mass per day. The settlement rate coefficient λ_s does not affect the steady state mat biomass or height (see "Steady state" below), only the rate at which the steady state is attained. Again, the value of $\lambda_s = 0.004$ m day^{-1} was chosen so that the mat was approximately at steady state within a 200 day period. We set the decay height to be $h_d = 0.05$ m as most of the biomass decay occurs at the plant's basal nodes, which are up to approximately 5 cm above ground level (James et al., 2015). Model behavior is insensitive to this parameter provided it is larger than the layer thickness δh, which we set as 0.002 m. Table 1 shows model variables and parameter values.

The system of differential equations (2) and (3) was initialized with

$$\rho_i = \begin{cases} 100\ \mathrm{g\ m^{-3}} & \text{if } i\,\delta h \le 0.1\ \mathrm{m}, \\ 0 & \text{otherwise.} \end{cases}$$

This represents a mat with a relatively low initial biomass and a height of 0.1 m. Different initial conditions produce the same long-term results, provided that initial conditions are such that the biomass per unit volume does not exceed the maximum biomass per unit volume in any layer. The equations were solved with Matlab's ordinary differential equation solver *ode45*.

Model results

Steady state. For the mat to reach steady state there must be no net production of biomass and the settlement terms must equal zero in each layer. No net production of biomass requires $\lambda_p \sum_{j=1}^{N} \rho_j l_j = k \sum_{j=1}^{N} \rho_j$. If the layer thickness δh is sufficiently small, the biomass in layer i can be approximated as a continuous function $\rho(x)$ of height x, where $x = i\delta h$, and the steady state condition may be written

$$\lambda_p \int_0^H \rho(x) \exp\left(-\mu \int_x^H \rho(y)\, dy\right) dx = k \int_0^H \rho(x)\, dx.$$

Evaluating the integrals and using M to denote the total plant biomass per unit area $\int_0^H \rho(x)dx$ gives

$$\frac{\lambda_p}{k\mu}(1 - e^{-\mu M}) = M.$$

This equation has two solutions for the steady state mat biomass: $M = 0$ and $M = M^*$. The nonzero steady state M^* is positive provided $\lambda_p/k > 1$. There is a transcritical bifurcation at $\lambda_p/k = 1$, and for $\lambda_p/k < 1$ the steady state M^* becomes infeasible ($M^* < 0$) and the zero steady state becomes stable. Since the value of λ_p is determined by the ambient light intensity, this bifurcation translates to a minimum light intensity required for viability of the mat. If the light intensity falls below this level, the mat is predicted to die.

The structure of the steady state equation above shows that the long-term biomass of the mat is determined only by the light absorption coefficient μ and the ratio of the photosynthesis to the respiration rate ratio λ_p/k, and is independent of the other model parameters and the shape of the vertical biomass profile $\rho(x)$. Hence the steady state results are robust to model assumptions about how biomass is distributed vertically within the mat. Increasing (or decreasing) the values of λ_p and k while maintaining a constant ratio means that the system evolves more rapidly (or slowly) to the same steady state.

Calculating the steady state mat height H from the steady state biomass M requires the vertical biomass profile $\rho(x)$ to be calculated. Consider the uppermost layer with non-zero biomass (i.e. such that $\rho_i > 0$ and $\rho_{i+1} = 0$). Since there is no settlement into the layer from above, there must be no settlement out of the layer. This can only be true if layer $i - 1$ is at its maximum biomass, $\rho_{i-1} = K_{i-1}$, which in turn requires $\rho_{i-2} = K_{i-2}$, and so on for all layers. Therefore, the steady state consists of a mat in which each layer is compressed to its maximum biomass (except possibly the uppermost non-empty layer). Again, approximating ρ_i by the continuous function $\rho(x)$, the biomass profile that satisfies the definition of K_i in Eq. (1) is

$$\rho(x) = c_0 e^{c_1(H-x)},$$

where H is the total height of the mat (i.e. the height of the uppermost non-empty layer). Substituting this profile into the equation $M = \int_0^H \rho(x)dx$ gives the steady state height H in terms of the total plant biomass M as

254 $$H = \frac{1}{c_1}\ln\left(1 + \frac{c_1 M}{c_0}\right).$$

255 Figure 3 shows how the steady state height H depends on the photosynthesis to respiration rate ratio
256 λ_p/k, showing the transcritical bifurcation at $\lambda_p/k = 1$. These results are qualitatively consistent with
257 field observations of Kelly and Skipworth (1984a) which suggested a minimum light intensity of around
258 0.5% of open ground for viability of the plant, and a mat biomass that increased linearly with light
259 intensity.

260 **Numerical results.** Figure 4 shows how the biomass and light intensity profiles evolve through time
261 for a mat above the critical ambient light intensity ($\lambda_p > k$). The mat initially has relatively low biomass
262 and a height of 10 cm (Fig. 4a). Through a combination of new biomass production and settlement,
263 the biomass quickly grows to the maximum biomass per unit volume in the 10 cm high mat (Fig. 4b).
264 Once this has occurred, the majority of new biomass production is confined to the uppermost layers
265 of the mat, where there is high light intensity and, more importantly, space to grow. Over time, this
266 new biomass causes compression of the mat, leading to increased biomass per unit volume in the
267 lower layers (Fig. 4c-e). As the total biomass increases, the net biomass production approaches zero
268 and the mat growth slows down (Fig. 4f). After 200 days, the mat height of 0.40 m and biomass profile
269 are close to the analytical steady state (dashed curve in Fig. 4f). The biomass profile is also consistent
270 with the range of experimental observations (open circles in Fig. 4f). Figure 5 shows a time series of
271 the total mat biomass; eventually, the total biomass reaches the analytical steady state biomass M^*
272 and the mat ceases to grow. If the ambient light intensity is below the critical level ($\lambda_p < k$), the
273 biomass reduces over time and eventually the mat shrinks to zero height and biomass.

274

275 **Discussion**

276 We have presented a simple model for the growth of a *Tradescantia fluminensis* mat, partly
277 parameterized using data on light intensity and biomass in experimentally grown mats. The model
278 predicts that the height of the mat formed by the plant depends on the ambient light level and there
279 is a critical light level below which the mat can no longer survive, which is consistent with field
280 observations (Kelly & Skipworth, 1984a). Unfortunately, the model could only be compared to the
281 data sampled at a single point in time in this experiment due to the destructive sampling methods
282 used. A larger scale experiment would be needed to quantitatively compare the model predictions
283 with data over time to enable the biomass compression model to be validated.

284 The experimentally grown mats reached dry biomass densities of 1294 – 2728 g m^{-2} and the model
285 was parameterized to be consistent with this. These biomass values are higher than field observations
286 of *T. fluminensis* in New Zealand: for example Kelly & Skipworth (1984a) recorded a mean dry biomass
287 of 455 g m^{-2} and a maximum of 1400 g m^{-2}. It is likely that the experimentally grown plants experienced
288 better growing conditions (regular watering, shelter from wind and frost, protection from herbivory)
289 than is typical in the field. In addition, the experimental setup meant that all new plant growth was
290 constrained to stay in the 0.5 m^2 container rather than being able to spread horizontally. This may
291 have led to higher biomass per unit area than would be seen in a comparable unconstrained mat.
292 Hence, to reproduce non-experimental conditions, it may be necessary to reduce the maximum
293 biomass density and the photosynthesis rate parameters.

294 The model is mathematically robust in that it is insensitive to initial conditions provided these are
295 ecologically sensible, e.g. starting with a top-heavy biomass profile may lead to spurious results. The
296 qualitative model predictions are also independent of the parameter values within reasonable ranges.

Given these caveats, the biomass profiles produced by the model are similar to those expected. The key prediction is that the mat will no longer be viable if the ambient light intensity drops to such a level that the plant's photosynthesis rate is less that its respiration rate. For the parameter values used in the numerical simulations, this would require a reduction in ambient light intensity by a factor of approximately 7. Kelly & Skipworth (1984a) observed that mat death only occurred when the light intensity was less than 4% of the light intensity of open ground. It is possible that, at high light levels, the plant's photosynthesis rate is a nonlinear function of light intensity and becomes limited by other variables such as nutrient availability. This hypothesis could be tested by performing experiments on mats with varying levels of shading. This would allow the model assumption on photosynthesis rate to be refined, resulting in more accurate predictions for the critical light intensity needed to make the mat non-viable.

Our model, which focuses on vertical structure within a horizontally uniform mat, is complementary to that of (Hogan & Myerscough, 2017), which focuses on horizontal spread of the mat. These two approaches could be combined to produce a model of interdependent vertical structure and horizontal spreading, which would lead to improved understanding of the plant's growth and spread. Another aspect worthy of inclusion in future work is the stochastic nature of plant growth. This can be seen in the variability of the experimental results (Figs. 1b and 4f), but is not possible to capture in a deterministic model of the type developed here. For example, the respiration rate k is variable among plants and is affected by temperature, tissue age, nitrogen content and atmospheric pollutants (Cannell & Thornley, 2000).

Reducing herbicide use whilst still controlling weeds is an important conservation goal (McAlpine et al., 2018). The aim of *T. fluminensis* control is often to reduce the mat height to facilitate native plant species regeneration (McAlpine et al., 2017). Our model provides a starting point for testing the effect of control methods including the various types of biocontrol that are being proposed for *T. fluminensis* in New Zealand where it is an established pest. The model presented here accounts only for total plant biomass. In low-light conditions, the plant could change its allocation of resources from root and stem towards more photosynthetic material. This would change the energy balance at the plant level and this could make shading a less effective control measure. To investigate this in more detail, the model could be extended to account for the different parts of the plant, e.g. stems, leaves, nodes and their prevalence at different heights. This would allow more detailed modelling of specific biocontrol methods (Fowler et al., 2013; James et al., 2015).

Acknowledgements

We thank Dave Conder and Ben Jeffries for assistance with experimental setup, equipment and data collection, and Dave Kelly for insight into the plant's ecology. This project was partly funded by the Foundation for Research, Science and Technology (now Ministry of Business, Innovation and Employment) and Manaaki Whenua Landcare Research Core Funding under the programme Beating Weeds II (C09X0905).

Variables	
Height of layer i above ground level	h_i
Biomass per unit volume in layer i	ρ_i
Maximum biomass per unit volume in layer i as a function of biomass above layer i	$K_i = c_0 + c_1 \delta h \sum_{j=i}^{N} \rho_j$
Relative light intensity in layer i	$l_i = \exp(-\mu \delta h \sum_{j=i}^{N} \rho_j)$
Constant parameters	
Photosynthesis rate coefficient	$\lambda_p = 0.1$ day^{-1}
Respiration rate coefficient	$k = 0.015$ day^{-1}
Settlement rate coefficient	$\lambda_s = 0.004$ m day^{-1}
Light absorption coefficient	$\mu = 0.00334$ m^2 g^{-1}
Maximum uncompressed biomass per unit volume	$c_0 = 2275.8$ g m^{-3}
Rate of biomass increase as a result of compression	$c_1 = 3.47$ m^{-1}
Layer thickness	$\delta h = 0.002$ m
Decay height	$h_d = 0.05$ m

Table 1. Model variables and parameter values used for numerical results. Note that the key model output, the total mat biomass M at steady state, depends only the light absorption coefficient μ and the photosynthesis to respiration rate ratio λ_p/k and is independent of other parameter values.

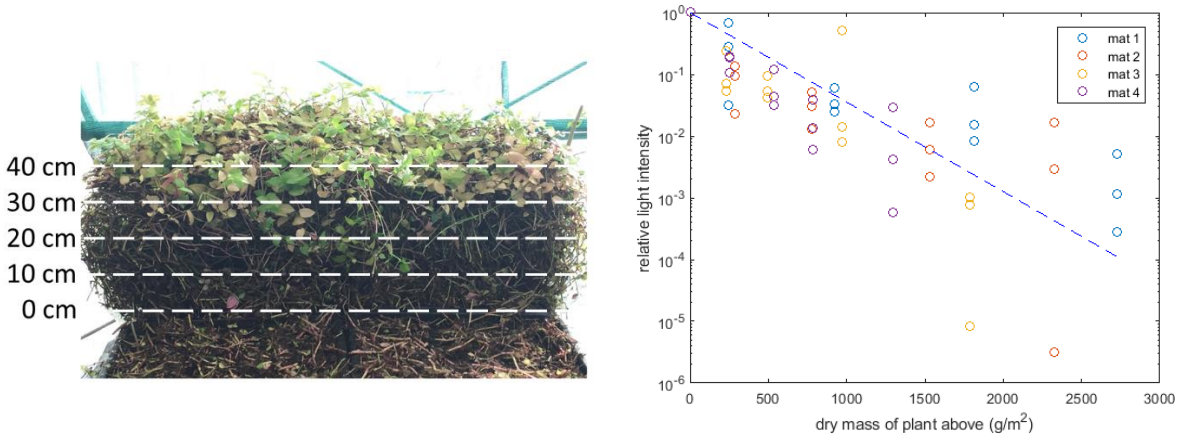

(a) (b)

Figure 1. Experimental setup and results. (a) Cross-section of one of four experimental replicate *T. fluminensis* mats ("mat 1") of approximately 40 cm height, shown part way through the biomass collection procedure. The total dry biomass in each of the four layers shown was measured. (b) Data on light intensity (relative to ambient) and total dry biomass above height 0, 10, 20, 30 and 40 cm from the four replicate mats. At each height and for each mat, there are three vertically aligned points corresponding to the three light intensity measurements; for each mat, height decreases from left to right (see Supplementary Material Table S1 for data). Dashed blue line shows fitted exponential relationship $\log(l) = -\mu w$ between light intensity (l) at a given height and biomass (w) above that height, with absorption coefficient $\mu = 0.00334$ m^2 g^{-1} ($p = 10^{-23}$, $r^2 = 0.57$).

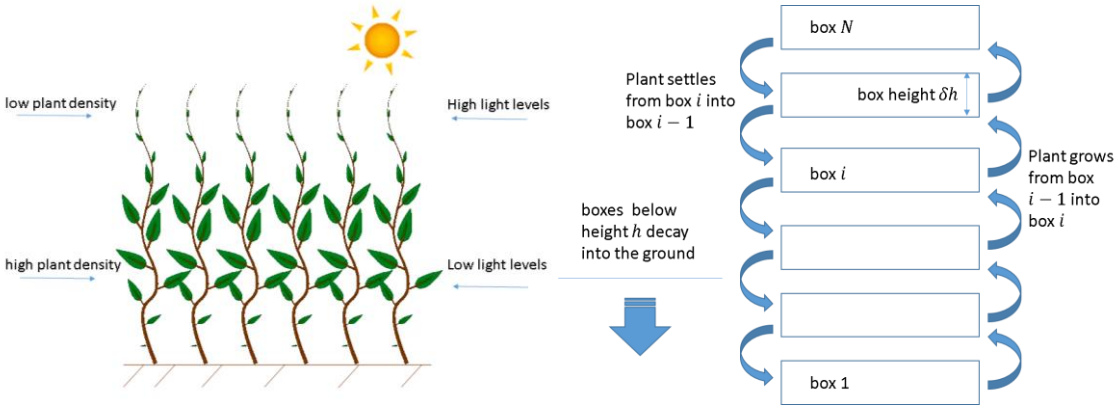

Figure 2. Schematic diagram showing the model of *T. fluminensis* mat biomass in thin horizontal layers.

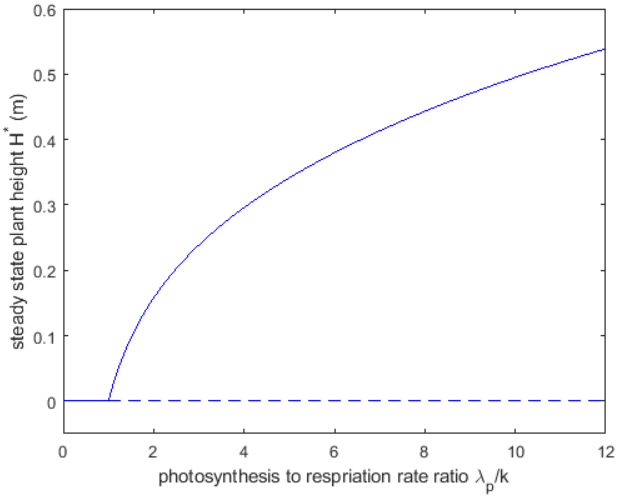

Figure 3: Bifurcation diagram showing the transcritical bifurcation. Steady state mat height H^* as a function of the photosynthesis to respiration rate ratio λ_p/k (stable = solid, unstable = dashed). As the plant's photosynthesis rate is reduced, for example due to a decrease in ambient light levels, the steady state height of the mat decreases. At some point it reaches a critical level where $\lambda_p/k = 1$ where it undergoes a transcritical bifurcation; if the photosynthesis rate is reduced so that $\lambda_p/k < 1$, the plant can no longer sustain itself and dies out.

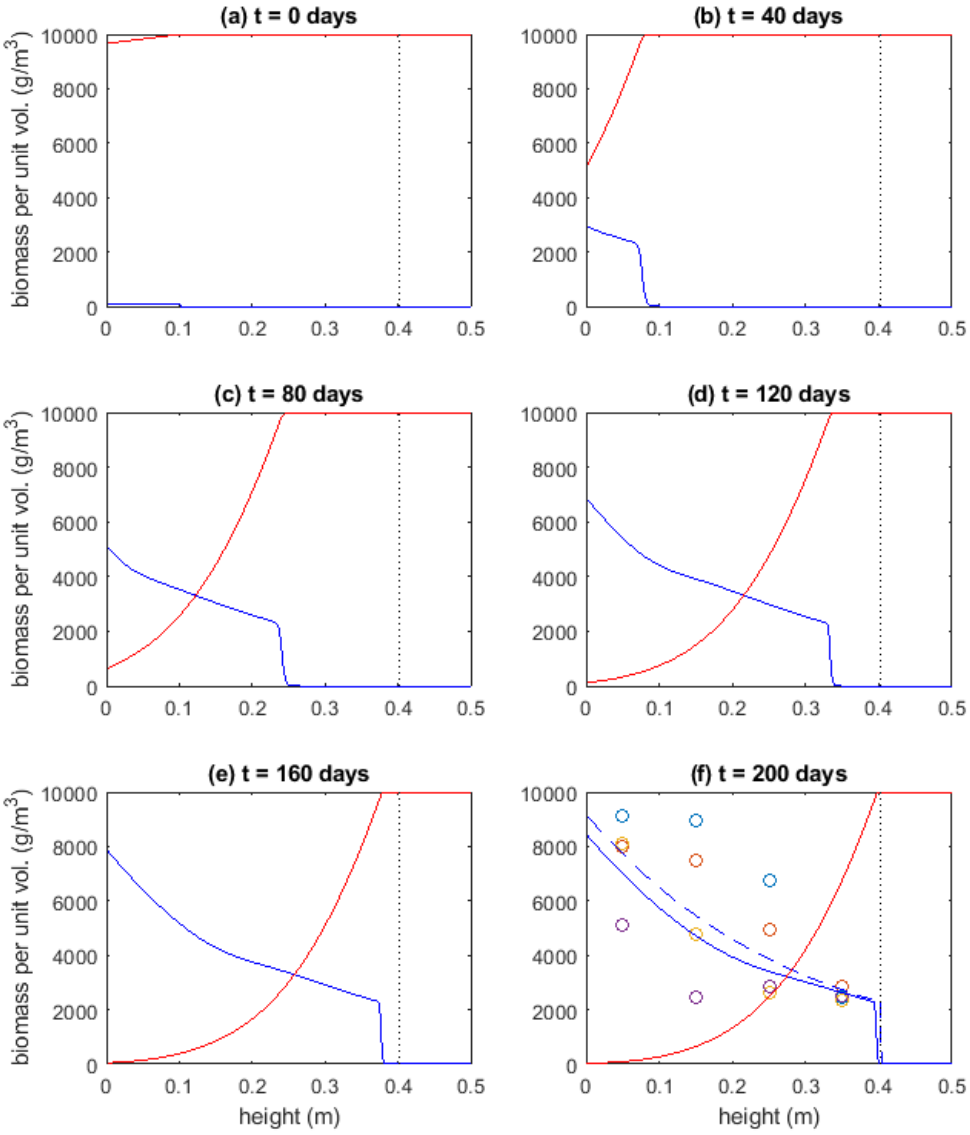

359

360 **Figure 4.** Growth of a mat when ambient light intensity is above the critical level ($\lambda_p > k$). Each graph
361 shows the vertical profile of plant biomass (solid blue) and relative light intensity (solid red) and
362 analytical steady state height H^* (dashed black). Panel (f) shows the analytical steady state biomass
363 profile (dashed blue) along with the experimental biomass measurements (open circles: blue = mat 1,
364 red = mat 2, yellow = mat 3, magenta = mat 4) made at that time. Initial conditions correspond to a
365 plant with biomass per unit volume 100 g m^{-3} and height 0.1 m. Parameter values as shown in Table
366 1.

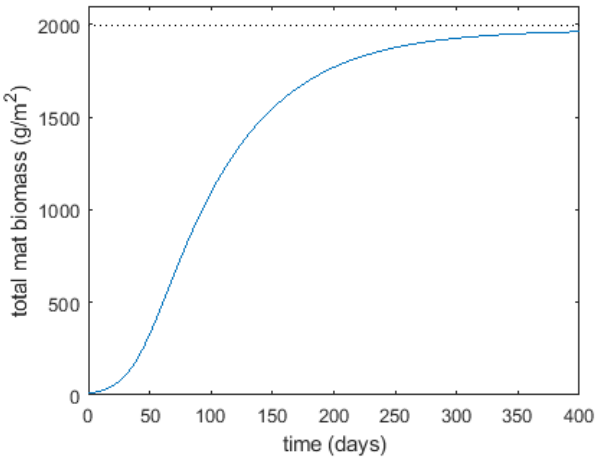

Figure 5. Time series of the total biomass M of the mat shown in Fig. 4. Horizontal dotted line shows the analytical steady state biomass M^*. Parameter values as shown in Table 1.

References

Adams, T. P., Holland, E. P., Law, R., Plank, M. J., & Raghib, M. (2013). On the growth of locally interacting plants: differential equations for the dynamics of spatial moments. *Ecology, 94*(12), 2732-2743.

Brunner, A. (1998). A light model for spatially explicit forest stand models. *Forest ecology and management,* 107, 19-46.

Burns, J. H. (2008). Demographic performance predicts invasiveness of species in the Commelinaceae under high-nutrient conditions. *Ecological Applications, 18*(2), 335-346.

Cannell, M. G. R., & Thornley, J.H.M. (2000). Modelling the components of plant respiration: some guiding principles. *Annals of Botany*, 85, 45-54.

Fowler, S. V., Barreto, R., Dodd, S., Macedo, D. M., Paynter, Q., Pedrosa-Macedo, J. H., . . . Waipara, N. (2013). Tradescantia fluminensis, an exotic weed affecting native forest regeneration in New Zealand: ecological surveys, safety tests and releases of four biocontrol agents from Brazil. *Biological Control, 64*(3), 323-329.

Hogan, A. B., & Myerscough, M. R. (2017). A Model for the Spread of an Invasive Weed, Tradescantia fluminensis. *Bulletin of Mathematical Biology, 79*(6), 1201-1217.

Jaeger, M., & De Reffye, P. (1992). Basic concepts of computer simulation of plant growth. *Journal of biosciences, 17*(3), 275-291.

James, A., Molloy, S. M., Ponder-Sutton, A., Plank, M. J., Lamoureaux, S. L., Bourdôt, G. W., & Kelly, D. (2015). Modelling Tradescantia fluminensis to assess long term survival. *PeerJ, 3*, e1013.

Kelly, D., & Skipworth, J. (1984a). Tradescantia fluminensis in a Manawatu (New Zealand) forest: I. Growth and effects on regeneration. *New Zealand Journal of Botany, 22*(3), 393-397.

Kelly, D., & Skipworth, J. (1984b). Tradescantia fluminensis in a Manawatu (New Zealand) forest: II. Management by herbicides. *New Zealand Journal of Botany, 22*(3), 399-402.

Maule, H., Andrews, M., Morton, J., Jones, A., & Daly, G. (1995). Sun/shade acclimation and nitrogen nutrition of Tradescantia fluminensis, a problem weed in New Zealand native forest remnants. *New Zealand Journal of Ecology*, 19(1), 35-46.

McAlpine, K. G., Lamoureaux, S. L., Timmins, S. M., & Wotton, D. M. (2017). Native woody plant recruitment in lowland forests invaded by non-native ground cover weeds and mammals. *New Zealand Journal of Ecology, 41*(1), 65-73.

McAlpine, K. G., Lamoureaux, S. L., Timmins, S. M., & Wotton, D. M. (2018). Can a reduced rate of herbicide benefit native plants and control ground cover weeds? *New Zealand Journal of Ecology, 42*(2), 204-213.

McAlpine, K. G., Lamoureaux, S. L., & Westbrooke, I. (2015). Ecological impacts of ground cover weeds in New Zealand lowland forests. *New Zealand Journal of Ecology, 39*(1), 50-60.

Perry, L. G., Neuhauser, C., & Galatowitsch, S. M. (2003). Founder control and coexistence in a simple model of asymmetric competition for light. *Journal of Theoretical Biology, 222*(4), 425-436.

Prusinkiewicz, P. (2004). Modeling plant growth and development. *Current opinion in plant biology, 7*(1), 79-83.

Scott, L. I., & Priestley, J. (1925). Leaf and Stem Anatomy of Tradescantia fluminensis, Vell. *Journal of the Linnean Society of London, Botany, 47*(312), 1-28.

Sellier, D., Plank, M. J., & Harrington, J. J. (2011). A mathematical framework for modelling cambial surface evolution using a level set method. *Annals of Botany, 108*(6), 1001-1011.

Standish, R. J. (2002). Experimenting with methods to control Tradescantia fluminensis, an invasive weed of native forest remnants in New Zealand. *New Zealand Journal of Ecology*, 26(2), 161-170.

Standish, R. J. (2004). Impact of an invasive clonal herb on epigaeic invertebrates in forest remnants in New Zealand. *Biological Conservation, 116*(1), 49-58.

Toft, R. J., Harris, R. J., & Williams, P. A. (2001). Impacts of the weed Tradescantia fluminensis on insect communities in fragmented forests in New Zealand. *Biological Conservation, 102*(1), 31-46.

420 Vance, R. R., & Nevai, A. L. (2007). Plant population growth and competition in a light gradient: a
421 mathematical model of canopy partitioning. *Journal of Theoretical Biology, 245*(2), 210-219.
422 YAN, H. P., Kang, M. Z., De Reffye, P., & Dingkuhn, M. (2004). A dynamic, architectural plant model
423 simulating resource-dependent growth. *Annals of Botany, 93*(5), 591-602.
424 Yeates, G. W., & Williams, P. A. (2001). Influence of three invasive weeds and site factors on soil
425 microfauna in New Zealand. *Pedobiologia, 45*(4), 367-383.

426